

This is an Open Access document downloaded from ORCA, Cardiff University's institutional repository: <https://orca.cardiff.ac.uk/id/eprint/129339/>

This is the author's version of a work that was submitted to / accepted for publication.

Citation for final published version:

Pawar, Sambhaji M., Pawar, Bharati S., Hou, Bo , Kim, Jongmin, Ahmed, Abu Talha Aqueel, Chavan, Harish. S., Jo, Yongcheol, Cho, Sangeun, Inamdar, Akbar I., Gunjekar, Jayavant L., Kim, Hyungsang, Cha, SeungNam and Im, Hyunsik 2017. Self-assembled two-dimensional copper oxide nanosheet bundles as an efficient oxygen evolution reaction (OER) electrocatalyst for water splitting applications. *Journal of Materials Chemistry A* 5 (25) , pp. 12747-12751. 10.1039/C7TA02835K

Publishers page: <http://dx.doi.org/10.1039/C7TA02835K>

Please note:

Changes made as a result of publishing processes such as copy-editing, formatting and page numbers may not be reflected in this version. For the definitive version of this publication, please refer to the published source. You are advised to consult the publisher's version if you wish to cite this paper.

This version is being made available in accordance with publisher policies. See <http://orca.cf.ac.uk/policies.html> for usage policies. Copyright and moral rights for publications made available in ORCA are retained by the copyright holders.



Self-assembled Two-dimensional Copper Oxide Nanosheet Bundles as an efficient Oxygen Evolution Reaction (OER) electrocatalyst for water splitting application

Sambhaji M. Pawar,^{*,†} Bharati S. Pawar,[†] Bo Hou,[‡] Jongmin Kim,[†] Abu Talha A. A.,[†] Harish. S. Chavan,[†] Yongcheol Jo,[†] Sangeun Cho,[†] Akbar I. Inamdar,[†] Jayavant L. Gunjekar,[†] Hyungsang Kim,[†] SeungNam Cha[‡] and Hyunsik Im^{*,†}

[†] Division of Physics and Semiconductor Science, Dongguk University, Seoul 04620, South Korea

[‡] Department of Engineering Science, University of Oxford, Parks Road, OX1 3PJ, UK

ABSTRACT: A high-activity of two-dimensional (2D) copper oxide (CuO) electrocatalyst for the oxygen evolution reaction (OER) is presented. The CuO electrode self-assembles on a stainless steel substrate via a chemical bath deposition at 80 °C in a mixed solution of CuSO₄ and NH₄OH, followed by air annealing treatment, and shows a 2D nanosheet bundle-type morphology. The OER performance is studied in a 1M KOH solution. The OER starts to occur at about 1.48 V versus RHE ($\eta = 250$ mV) with a Tafel slope of 59 mV/dec in a 1M KOH solution. The overpotential (η) of 350 mV at 10 mA/cm² is among the lowest compared with other copper-based materials. The catalyst can deliver a stable current density of > 10 mA/cm² for more than 10 hours. This superior OER activity is due to its adequately exposed OER-favorable 2D morphology and the optimized electronic properties resulting from the thermal treatment.

KEYWORDS: *self-assembled CuO nanosheet, Chemical bath deposition, electrocatalyst, oxygen evolution reaction*

Corresponding Author

*E-mail: spawar81@gmail.com (S.M.P.), hyunsik7@dongguk.edu (H.I.)

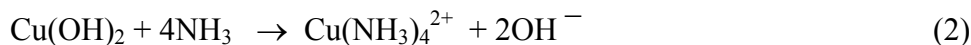
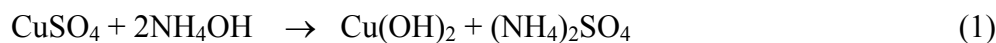
The electrochemical water splitting into hydrogen and oxygen provides the most promising and sustainable approach to produce clean hydrogen fuel using electricity generated from the renewable energy sources, such as solar energy, wind power and hydropower.^{1,2} Electrochemical water splitting processes generally involve two half-reactions: the hydrogen evolution reaction (HER) at the cathode, and the oxygen evolution reaction (OER) at the anode.³ Both the HER and OER reactions are crucial for the overall water splitting efficiency. However, the H₂ production from electrocatalytic water splitting is seriously restricted by the sluggish kinetics of the OER on the anode and it also requires a greater overpotential than the theoretical potential of 1.23 V.⁴ So far, iridium and ruthenium oxides (IrO₂ and RuO₂) are the most active OER electrocatalysts because of their excellent OER performance in acidic as well as alkaline media.^{5,6} However, the high cost and low abundance of these materials limit their large-scale applications. Hence, development of efficient, inexpensive and earth abundant OER electrocatalysts with a low overpotential are highly desired to make the whole water splitting reaction more energy-efficient.

In recent years, considerable attention has been focused on the first row transition metals-based oxide materials for electrochemical water splitting applications.⁷⁻⁹ Especially, there has been increasing interest in Cu-based water oxidation catalysts due to their high abundance, low cost and rich redox properties.¹⁰ Various Cu-based nanostructured oxides have been demonstrated as water splitting electrocatalysts. However, their **onset overpotential** values are still high ranging between 320 - 450 mV, and Tafel slope is between 95 - 44 mV/dec.¹⁰⁻¹⁷ Among various nanostructures, two-dimensional (2D) nanostructures can provide the most ideal morphological foundation for highly-active electrocatalyst because of their significantly shortened ion and electron diffusion pathways, large electrochemical active sites and electrode-

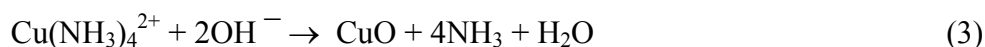
electrolyte interface, and improved structural stability, etc.¹⁸⁻²⁰ In this work, a self-assembled 2D CuO nanosheet bundle-type film has been synthesized for water splitting applications using a chemical bath deposition technique, which is facile and economically feasible for the synthesis of high-quality CuO films on a large surface area at low temperatures.²¹ The 2D CuO nanosheet electrode exhibits superior overall performance such as a remarkably low onset overpotential ($\eta = 250$ mV) and good Tafel slope of 59 mV/dev, compared to previously-studied Cu-based electrocatalysts and many inorganic materials.

The 2D CuO nanosheet bundle-type electrode film was fabricated via the chemical bath deposition on stainless substrate using a mixed solution of 0.1M CuSO₄ and 1M NH₄OH. Because stainless steel is cost-effective, highly conductive, and very stable in most acids and alkaline solutions, it may serve as an ideal substrate for large-scale OER applications. During the deposition, the pH of the solution was maintained at ~ 13 . A cleaned stainless steel substrate was immersed in the bath containing the solution, and the temperature was maintained at 80 °C for 6 hours. A heterogeneous reaction occurred, and the 2D nanostructured CuO was deposited on the substrate.

For the synthesis of the 2D CuO nanosheet bundles, two distinct steps are involved; i.e., nucleation and subsequent particle growth. 3 mL of the NH₄OH solution is added into the CuSO₄ solution to form a Cu(OH)₂ precipitate. When the amount of the NH₄OH solution is increased from 3 mL to 5 mL, the Cu(OH)₂ precipitate is dissolved at a pH value ~ 12 producing complex Cu(NH₃)₄²⁺ ions and a clear solution is obtained. Well aligned 2D CuO nanosheets are obtained by reducing the rate of the crystal growth as well as the spontaneous precipitation that are controlled by increasing the pH from 12 to 13.



When this solution bath is heated to 80 °C, the ionic product starts to exceed the solubility product by releasing H₂O and NH₃, and highly anisotropic positively charged CuO nuclei are formed on the substrate surface as well as in the solution:



These CuO nuclei assemble together to form thermodynamically unstable nanostrand structures with a high aspect ratio.^{22,23} They serve as ideal building blocks and tend to self-assemble into 2D nanosheets. The individual nanosheet has a higher surface energy and therefore it tends to aggregate perpendicularly to the surface plane.²⁴ As the reaction proceeds further, the thin 2D nanosheets self-aggregate to form bundles of nanosheets on the substrate for the minimizing of the overall surface energy.

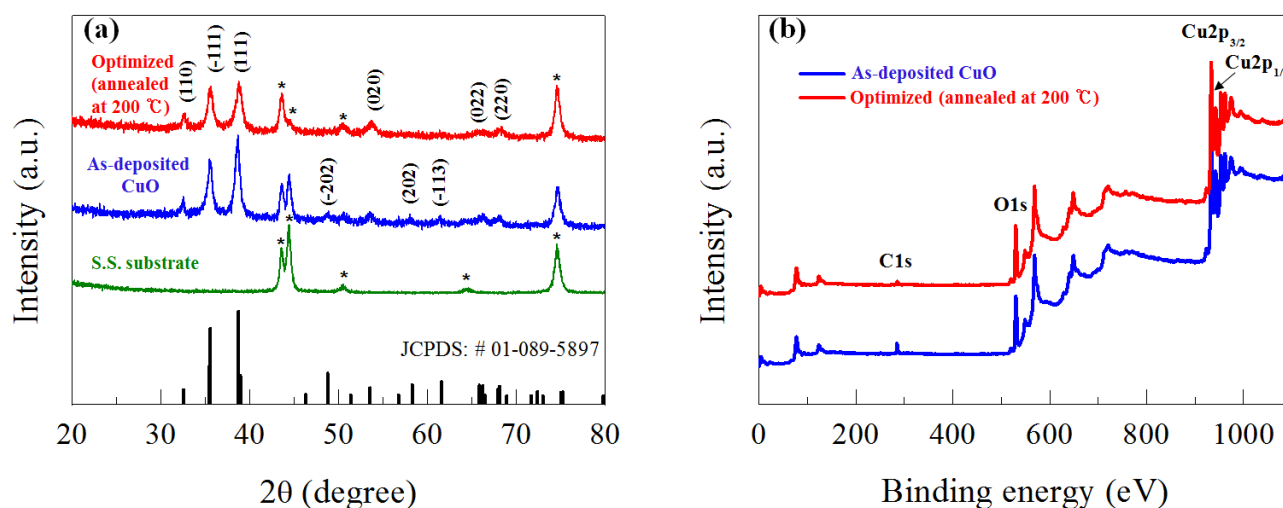


Figure 1: (a) X-ray diffraction patterns and (b) full-scale XPS spectra of the as-deposited and optimized 2D CuO nanosheet bundle films.

Figure 1(a) shows the XRD patterns of the as-deposited and optimized (annealed at 200 °C) 2D CuO nanosheets. The films show major diffraction peaks at 32.50° , 35.54° , 38.60° , 53.52° , 66.19° and 68.15° which correspond to the (110), (-111), (111), (020), (022) and (220) planes, respectively, of a polycrystalline monoclinic CuO structure (JCPDS No. # 01-089-5897). The diffraction peaks with the asterisk (*) are linked to the stainless steel substrate. The Cu(OH)₂ and Cu₂O phases are not detected in the XRD spectra. Using the Scherer's formula,²⁵ the average crystallite size for the as-deposited 2D CuO nanosheet films is found to be ~ 13 nm, whereas after annealing, it decreases to ~ 10 nm (Figure S1).

Figure 1(b) shows the full-scale XPS spectra of the 2D CuO nanosheet films. Typical carbon (C1s), oxygen (O1s) and copper (Cu2p_{1/2, 3/2}) signals are detected at around 285 eV, 530 eV and 935~955 eV respectively (see Figure S2 in the supplementary information for the enlarged peaks for each signal). The small non-oxygenated carbon (C1s) peak is a referenced peak. Two Cu2p peaks, Cu2p_{3/2} and Cu2p_{1/2}, are observed at 933.96 eV and 953.92 eV respectively. Additional shake-up peaks are also detected with a binding energy of ~10 eV higher than that of the main Cu2p_{3/2} and Cu2p_{1/2} peaks, due to the existence of an unfilled Cu3d₉ shell.²⁶ A shoulder-like feature at 531 eV is detected near the O1s peak at 529.7 eV, and this is attributed to surface-bound hydroxide species that originate from the adsorbed H₂O molecules on the surface.^{16,27}

Figure 2 (a and d) shows the SEM images of the 2D CuO nanosheet electrode films. The annealing of the as-prepared CuO nanosheet film does not affect its morphology. The morphology has well-defined uniform 2D nanosheet bundles, and each bundle contains 20 to 30 compact 2D CuO nanosheets that are grown vertically on the substrate surface. The thickness (*t*)

and length (L) of each nanosheet are 10-15 nm and 1-2 μm respectively (Figure S3). These nanosheet bundles self-aggregate randomly covering the whole surface of the substrate. EDS analysis (Table S1) reveals that whilst the as-prepared sample is slightly oxygen-rich presumably due to the hydroxide content in the film and the optimized sample annealed at 200 $^{\circ}\text{C}$ becomes copper-rich.

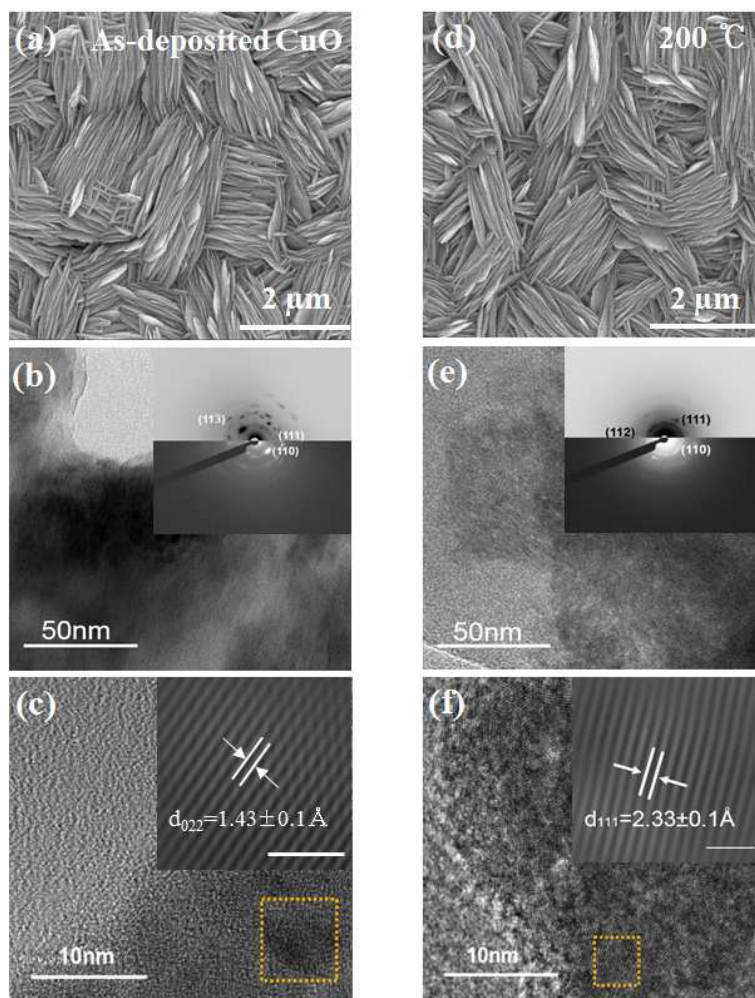


Figure 2: (a,d) FE-SEM images of the as-deposited and optimized (annealed at 200 $^{\circ}\text{C}$) nanosheet films, respectively. (b,c) TEM and HRTEM images of the as-deposited 2D CuO nanosheet film, respectively. (e,f) TEM and HRTEM images of the optimized 2D CuO nanosheet film, respectively. The insets in (b) and (e) show the SAED patterns. The insets in (c) and (f) show the magnified images of the selected area of the HRTEM images with a scale bar of 1 nm.

Figure 2 (b and e) shows the TEM images of the as-deposited and optimized 2D CuO nanosheets scratched off from the substrate. The insets show the selected area electron diffraction (SAED) patterns. The observed diffraction spots with diffused rings suggest that the sample is polycrystalline. The high resolution TEM (HRTEM) images (see Figure 2(c and f)) show clear lattice fringes with an interplanar spacing of 1.43Å and 2.33Å that correspond to the (022) and (111) plane of the monoclinic crystal structure of CuO. As the annealing temperature is increased to 300 °C, the crystallinity of the CuO nanosheets becomes degenerated (see Figure S4 in the Supplementary Information), which can be revealed by the broaden peaks in the XRD results and diffused rings in SAED.²⁸

The OER activities of the as-deposited and optimized 2D CuO nanosheet electrodes are investigated using liner sweep voltammetry (LSV) at a scan rate of 10 mV/s in 1M KOH and 0.2M borate buffer solutions and are shown in Figure 3(a) and Fig. S5. Both the electrodes exhibit a remarkably low onset overpotential of 270 mV for the as-deposited sample and 250 mV for the optimized sample in a 1M KOH solution. A low overpotential of 380 mV and 350 mV is required to drive a current density of 10 mA/cm² respectively. However, for the samples annealed at 100 °C and 300 °C, their overpotential values are slightly larger (Figure S6). On the other hand, it requires an overpotential of 543 mV to drive a current density of 1 mA/cm² in a 0.2M borate buffer solution. Relatively higher catalytic activity of the 2D nanosheet electrode is observed in a KOH solution rather than borate buffer solution. These values are considerably lower than those obtained from other Cu-based oxide electrocatalysts (see Table S2). The superior catalytic activity of the optimized CuO nanosheet electrode could be attributed to its

unique OER-favorable 2D morphology and the improved electronic properties resulting from the thermal treatment.

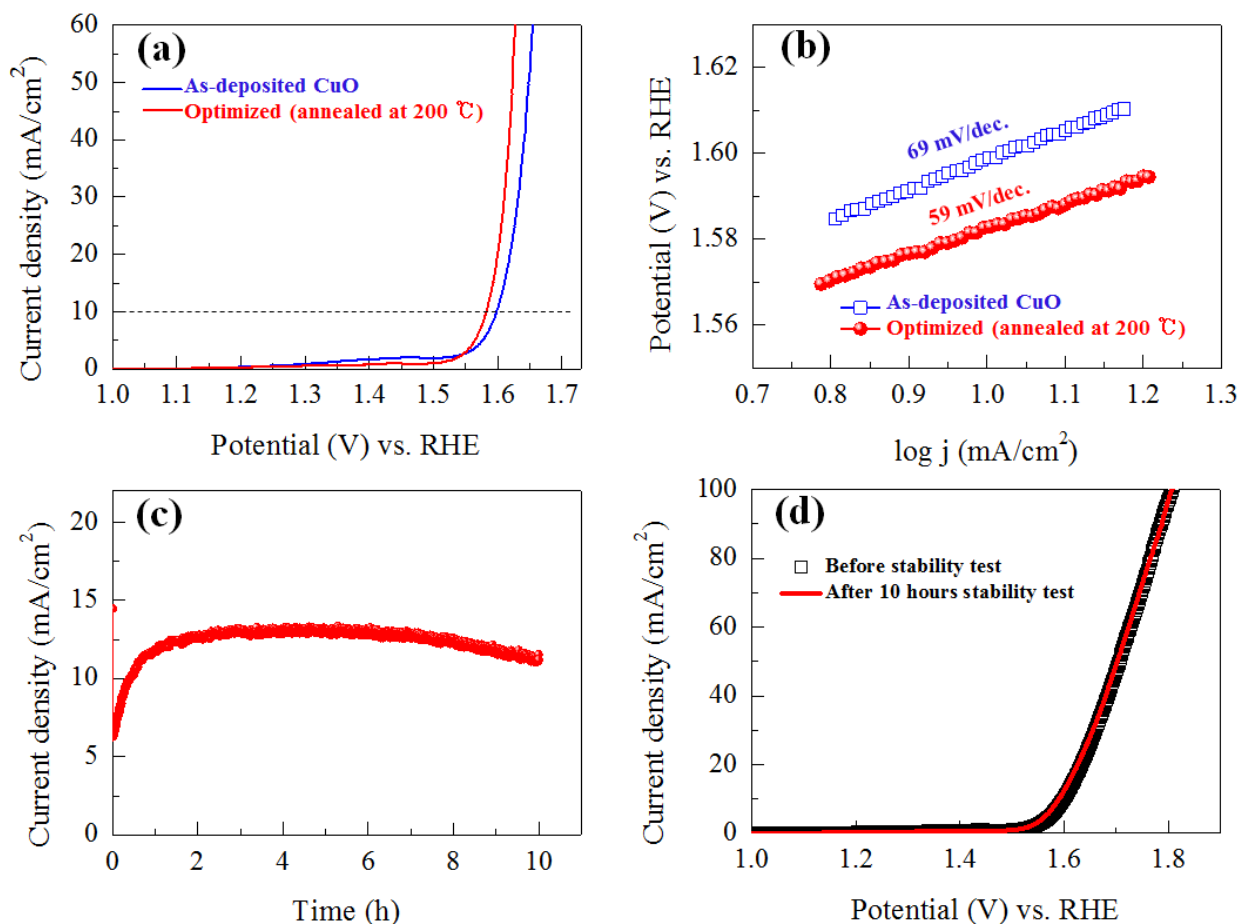


Figure 3: Electrochemical OER performance in 1 M KOH: (a) OER LSV curves (iR-compensated) of the 2D CuO nanosheet electrocatalysts (scan rate: 10 mVs⁻¹), (b) Tafel curves, (c) chronoamperometry stability test measured at 1.58 V vs. RHE, and (d) LSV curves of the optimized 2D CuO nanosheet electrode before and after the stability test.

Figure 3(b) shows the Tafel plot of the 2D CuO nanosheet electrodes. The linear portion of the Tafel curve is fitted using the Tafel equation $\eta = a + b \log j$, where η is the overpotential, a is the fitting parameter, and j is the current density and b is the Tafel slope. The Tafel slope of the as-deposited and optimized 2D CuO nanosheet electrode is 69 mV/dec. and 59 mV/dec. respectively, and this suggests that the optimized CuO electrode has improved reaction kinetics for OER. The long-term electrochemical stability of the CuO nanosheet electrode for the OER is also tested at a static potential of 1.58 V vs. RHE (see Figure 3(c)). The current density increases initially due to the activation process, producing high oxidation intermediates,¹¹ and then it remains stable over 10 hours. A vigorous and continuous gas evolution is observed on the surface during the stability measurement, and the gas bubbles dissipate rapidly into the electrolyte. The almost identical LSV curves (without an iR correction) of the optimized electrode before and after the stability test (Figure 3(d)) reveal its excellent durability for the OER in an extremely alkaline solution. XRD, XPS and SEM measurements are also performed after the stability measurements (See Fig. S7, Fig. S8 and Fig. S9 in the supporting information). There are no noticeable changes in the structural, morphological and compositional properties of the CuO electrocatalyst, suggesting that the CuO nanosheet bundle electrode is stable in alkaline KOH and 0.2M borate buffer solutions.

Figure 4 shows the EIS spectra of the 2D CuO nanosheet electrodes. The EIS spectra show a semi-circular feature in the high-frequency region and a straight line in the low-frequency region. This high-frequency semicircle is attributed to the charge-transfer resistance (R_{ct}) that is caused by the redox reaction that occurs on the surface of the electrocatalyst electrode, and the straight line is ascribed to the diffusion of the electrolyte within the electrode.²⁹

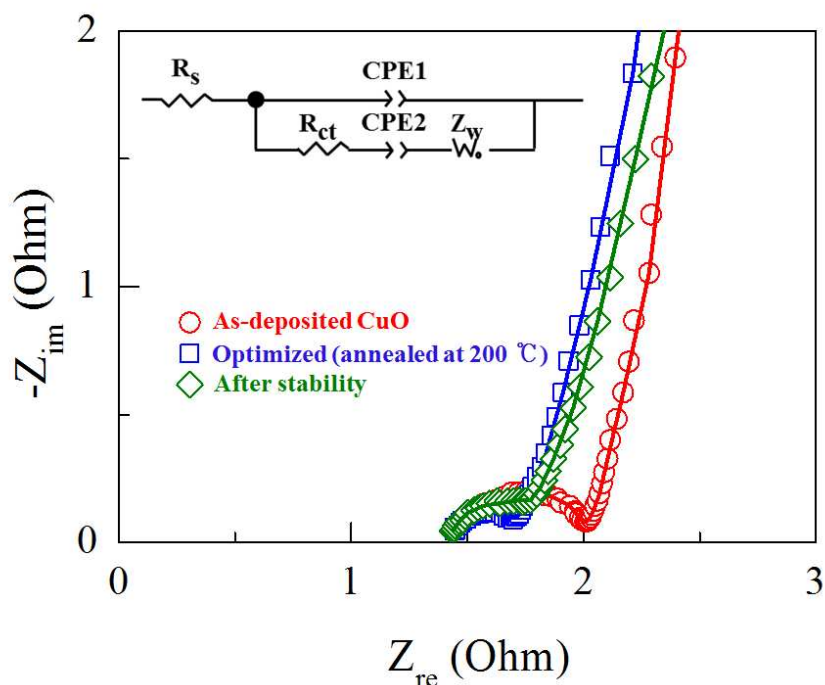


Figure 4: EIS spectra for the as-deposited and optimized 2D CuO electrocatalyst before and after the stability test. The inset shows the equivalent circuit for the simulation.

The equivalent series resistance (ESR) for the CuO nanosheet electrode is the combination of the ionic resistance of the electrolyte (R_s) and the R_{ct} in the electron transfer process of the electrode. The ESR values of the as-deposited and annealed CuO nanosheet electrodes are 2 Ω and 1.70 Ω , implying that the optimized 2D CuO nanosheets electrode has an enhanced charge-transfer rate and an improved catalytic activity. However, after the stability measurement, the ESR value increases by 10 % to 1.80 Ω .

In conclusion, a self-assembled 2D CuO nanosheet electrode film is synthesized using a chemical bath deposition method in a highly alkaline solution, and its OER performance is optimized by a heat treatment. The optimized 2D CuO nanosheet electrode shows the lowest onset overpotential of 250 mV with a Tafel slope \sim 59 mV/dec in a 1M KOH electrolyte solution.

The OER activity of the optimized 2D CuO nanosheets electrocatalyst shows a very low overpotential of 350 mV for the achievement of 10 mA/cm² and an excellent electrochemical stability. The superior catalytic activity and stability, along with the facile, easy and scalable fabrication process of the self-assembled 2D CuO nanosheet film offer a promising approach to the potential use of the electrode as an inexpensive catalyst material for electrochemical water splitting applications.

ACKNOWLEDGMENTS

The authors would like to thank the financial support from the National Research Foundation (NRF) of Korea (Grant nos. 2016R1A6A1A03012877, 2015M2A2A6A02045251, 2015R1A2A2A01004782, 2015R1D1A1A01058851 and 2015R1D1A1A01060743).

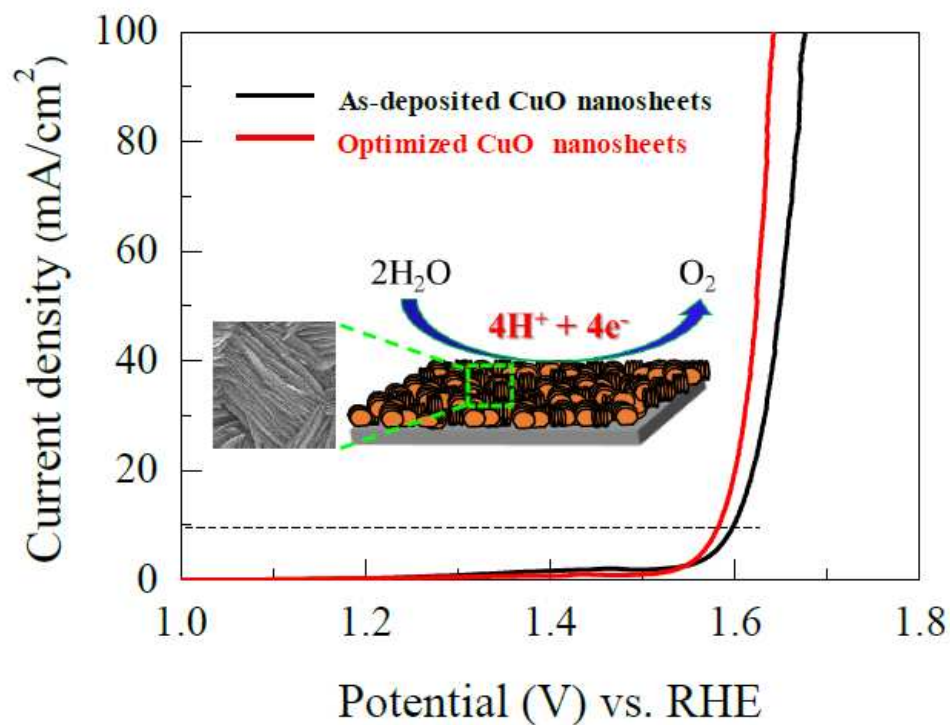
REFERENCES

- 1 M. G. Walter, E. L. Warren, J. R. McKone, S. W. Boettcher, Q. Mi, E. A. Santori and N.S. Lewis, *Chem. Rev.*, 2010, **110**, 6446.
- 2 Y. Li and C. Zhao, *Chem. Mater.*, 2016, **28**, 5659.
- 3 J. Wang, W. Cui, Q. Liu, Z. Xing, A. M. Asiri and X. Sun, *Adv. Mater.*, 2016, **28**, 215.
- 4 K. Zeng and D. Zhang, *Progress in Energy and Combustion Science*, 2010, **36**, 307.
- 5 T. Audichon, T.W. Napporn, C. Canaff, C. Morais, C. Comminges and K.B. Kokoh, *J. Phys. Chem. C*, 2016, **120**, 2562.
- 6 Y. Gorlin and T.F. Jaramillo, *J. Am. Chem. Soc.*, 2010, **132**, 13612.
- 7 I. Roger and M. D. Symes, *J. Mater. Chem. A*, 2016, **4**, 6724.
- 8 M. I. Jamesh, *Journal of Power Sources*, 2016, **333**, 213.
- 9 H. Osgood, S. V. Devaguptapu, H. Xu, J. Cho and G. Wu, *Nano Today*, 2016, **11**, 601.
- 10 X. Liu, S. Cui, Z. Sun, Y. Ren, X. Zhang and P. Du, *J. Phys. Chem. C*, 2016, **120**, 831.
- 11 S. Cui, X. Liu, Z. Sun and P. Du, *ACS Sustainable Chem. Eng.*, 2016, **4**, 2593.
- 12 N. Cheng, Y. Xue, Q. Liu, J. Tian, L. Zhang, A. M. Asiri and X. Sun, *Electrochimica Acta*, 2015, **163**, 102.
- 13 X. Liu, S. Cui, Z. Sun and P. Du, *Electrochimica Acta*, 2015, **160**, 202.
- 14 X. Liu, S. Cui, M. Qian, Z. Sun and P. Du, *Chem. Commun.*, 2016, **52**, 5546.
- 15 A. D. Handoko, S. Deng, Y. Deng, A.W. F. Cheng, K.W. Chan, H.R. Tan, Y. Pan, E.S. Tok, C. H. Sow and B.S. Yeo, *Catal. Sci. Technol.*, 2016, **6**, 269.
- 16 K.S. Joya and Huub J. M. de Groot, *ACS Catal.*, 2016, **6**, 1768.
- 17 F. Yu, F. Li, B. Zhang, H. Li and L. Sun, *ACS Catal.*, 2015, **5**, 627.

- 18 Z. Sun, T. Liao, Y. Dou, S. M. Hwang, M.-S. Park, L. Jiang, J.H. Kim and S.X. Dou, *Nature Commun.*, 2014, **5**, 3813.
- 19 B. Mendoza-Sánchez and Y. Gogotsi, *Adv. Mater.*, 2016, **28**, 6104.
- 20 Y. Tong, J. Xu, H. Jiang, F. Gao and Q. Lu, *Chemical Engineering Journal*, 2017, **316**, 225.
- 21 S. M. Pawar, B. S. Pawar, J. H. Kim, Oh-Shim Joo and C. D. Lokhande, *Current Applied Physics*, 2011, **11**, 117.
- 22 I. Ichinose, K. Kurashima and T. Kunitake, *J. Am. Chem. Soc.*, 2004, **126**, 7162.
- 23 V. R. Shinde, H.-S Shim, T.P. Gujar, H.J. Kim and W.B. Kim, *Adv. Mater.*, 2008, **20**, 1008.
- 24 L.-X. Yang, Y.-J. Zhu, H. Tong, Z.-H. Liang and W.-W. Wang, *Crystal Growth & Design*, 2007, **7**, 2716.
- 25 J. Kim, C. Park, S. M. Pawar, A. I. Inamdar, Y. Jo, J. Han, J. P. Hong, Y. S. Park, D. -Y. Kim, W. Jung, H. Kim and H. Im, *Thin Solid Films*, 2014, **566**, 88.
- 26 D. P. Dubal, G. S. Gund, R. Holze and C. D. Lokhande, *Journal of Power Sources*, 2013, **242**, 687.
- 27 A. C. Nwanya, D. Obi, K. I. Ozoemenad, R. U. Osuji, C. Awada, A. Ruediger, M. Maaza, F. Rosei, and F.I. Ezema, *Electrochimica Acta*, 2016, **198**, 220.
- 28 B. Hou, D. Parker, G. P. Kissling, J. A. Jones, D. Cherns, D. J. Fermin, *J. Phys. Chem. C*, 2013, **117**, 6814.
- 29 S. M. Pawar, B. S. Pawar, A. I. Inamdar, J. Kim, Y. Jo, S. Cho, S. S. Mali, C. K. Hong, J. Kwak, H. Kim and H. Im, *Materials Letters*, 2017, **187**, 60.
- 30 J. Du, Z. Chen, S. Ye, B. J. Wiley, and T. J. Meyer, *Angew. Chem. Int. Ed.*, 2015, **54**, 2073.
- 31 X. Ma, X. Li, A. D. Jagadale, X. Hao, A. Abudula and G. Guan, *Int. Journal of Hydrogen Energy*, 2016, **41**, 14553.

Table of content

Self-assembled CuO nanosheet Bundles for high-activity OER



The self-assembled CuO nanosheet bundles are fabricated on stainless steel via chemical bath deposition and optimized for efficient electrocatalysis. The superior activity for OER, outperforming the current Cu-based oxide electrocatalysts, is due to the unique OER-favorable 2D morphology and the facilitated electron transport resulting from the thermal treatment.

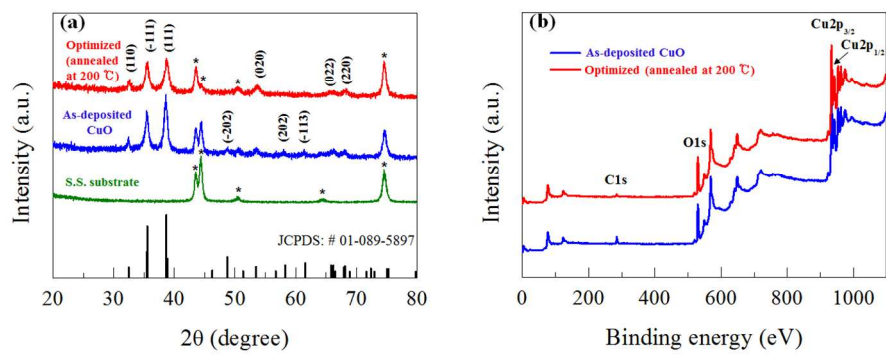


Fig.1

Figure 1

398x221mm (96 x 96 DPI)

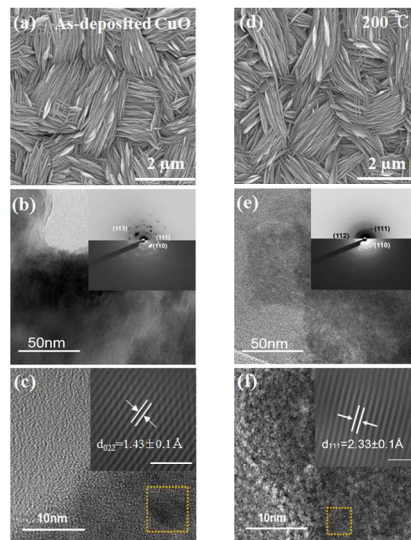


Fig.2

Figure 2

390x219mm (96 x 96 DPI)

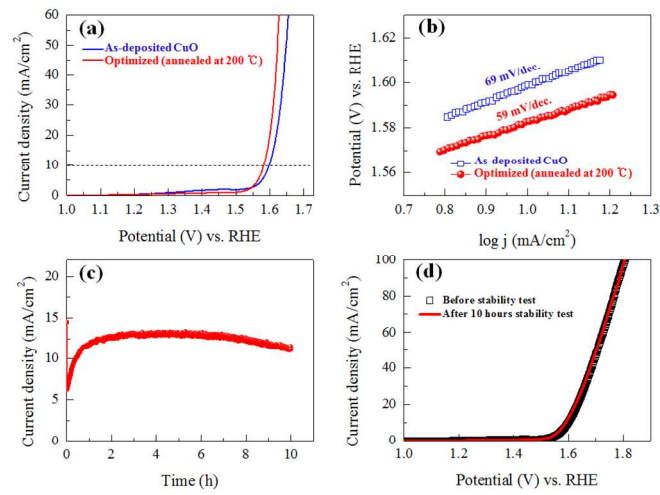


Fig.3

Figure 3

393x219mm (96 x 96 DPI)

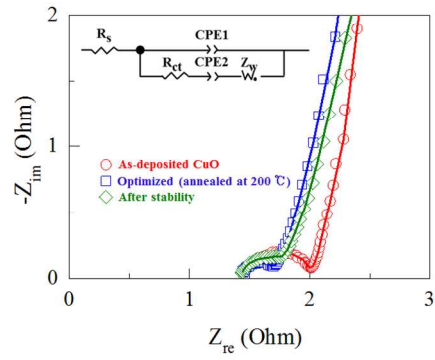


Fig.4

Figure 4

391x221mm (96 x 96 DPI)